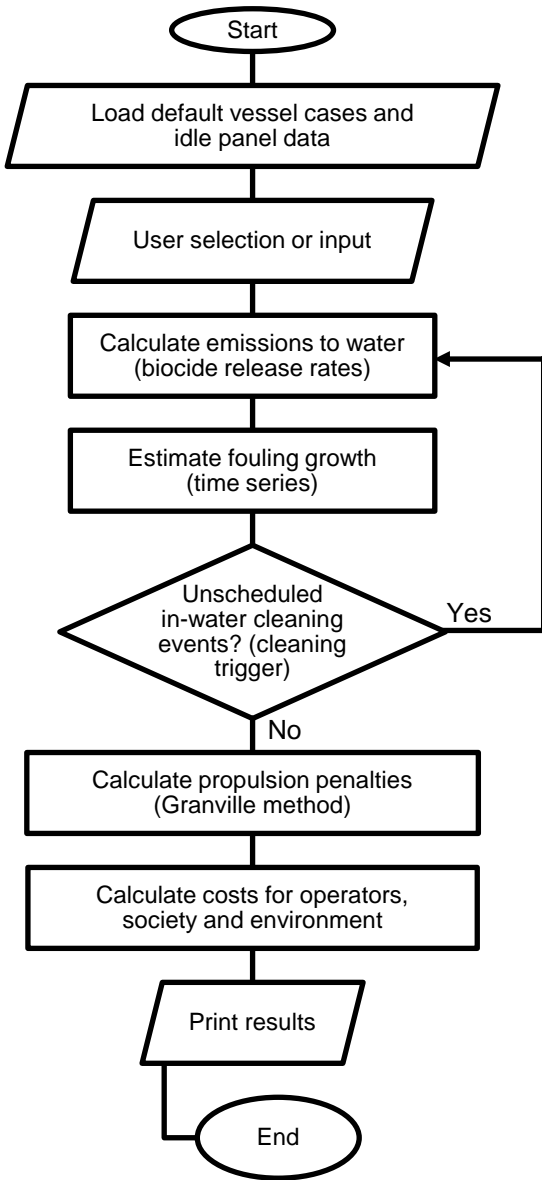


Supplementary materials

Supplementary Materials: Tool Flowchart and User interface



(a)

A1. Select vessel case:

Vessel case & details

Preview power-speed curves (optional)

Custom

- Bulk carrier, 0-9999 dwt
- Bulk carrier, 10000-34999 dwt
- Bulk carrier, 35000-99999 dwt
- Bulk carrier, 60000-99999 dwt

Length Between Perpendiculars [m]: 123.940

Breadth [m]: 15.870

Displacement [m³]: 12558

Main engine(s) MCR [kW]: 3840

Service speed [knots]: 13

Propulsive efficiency [-]: 0.70

Average transport work based on:

- Cargo [metric tons] = 9957
- Passengers [pax] = 0

MAKE current vessel details "Custom"

A2. Confirm details for energy carrier, main engines, and exhaust after-treatment:

Energy carrier: Heavy Fuel Oil (HFO)

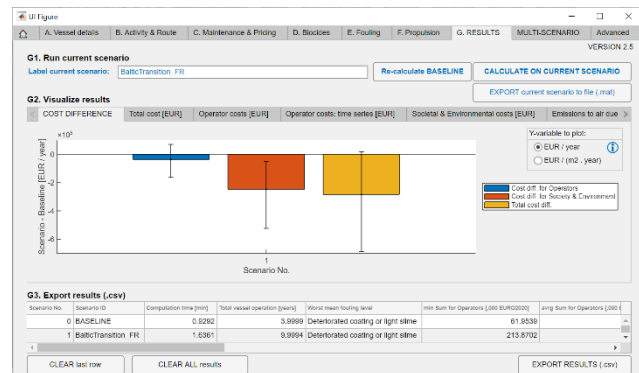
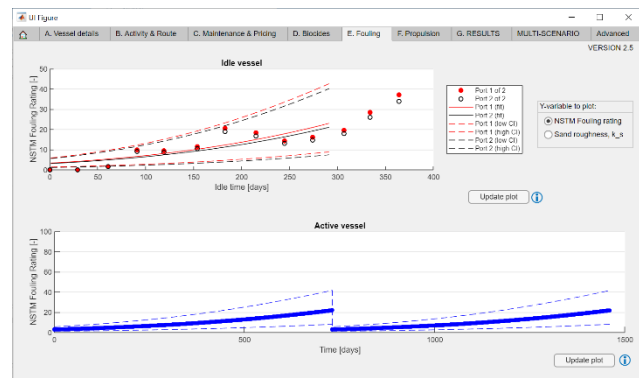
Specific Fuel Consumption (SFC): with max. sulfur content [t] = 0.07

Lower calorific value [MJ/kg]: 40.200

Selected Fuel: ULGSD

NOx reduction techniques

LOAD entire scenario from file (.mat)



(b)

HullMASTER's generic simulation approach (a) and example screens from user interface (b), from top to bottom: user input/selection (vessel details), intermediate results (time series for hull fouling rating), and final cost difference results.

*Supplementary Materials: Economic Social and Environmental Valuation
(pricing)*

Please refer to attached Excel spreadsheet (.xlsx).

Supplementary Materials: list of default vessels

Within each vessel class, a representative IMO-registered vessel has been selected, based on the median value for Maximum Continuous Rating (MCR), i.e. the installed power for propulsion. Vessel details for IMO-registered vessels were obtained from an international vessel registry (IHS Markit, 2020). The current selection of default vessels is not intended to accurately represent every specific vessel operating in the Baltic Sea region. Instead, the goal with such default list of vessels is to simply give the generic user a convenient starting point, offering a range of realistic vessel particulars, based on existing vessels. Additionally, nine vessels are currently added to this list (vessels A-I), which are used as validation cases. For these vessels, in-service performance data was kindly made available by their shipping operators, with operations in the Baltic Sea region (please refer to **Error! Reference source not found.**).

Case	Ship type (IMO 2020)	Ship type (IHS Markit)	Size category	Unit	Median main engine MCR [kW]	IMO number	Built
1	Bulk carrier	BULK CARRIERS	0–9999	dwt	1177	9048500	1992
2	Bulk carrier	BULK CARRIERS	10000–34999	dwt	5854	9289855	2003
3	Bulk carrier	BULK CARRIERS	35000–59999	dwt	8208	9301756	2007
4	Bulk carrier	BULK CARRIERS	60000–99999	dwt	9660	9740811	2016
5	Bulk carrier	BULK CARRIERS	100000–199999	dwt	16860	9476642	2012
6	Bulk carrier	BULK CARRIERS	200000–+	dwt	18623	9304942	2007
7	Chemical tanker	-Chemical	0–4999	dwt	1177	9231066	2000
8	Chemical tanker	-Chemical	5000–9999	dwt	3000	9479802	2010
9	Chemical tanker	-Chemical	10000–19999	dwt	4519	9321457	2006
10.1	Chemical tanker	-Chemical	20000–39999	dwt	7877	9259903	2003
10.2	Chemical tanker	-Chemical	40000–+	dwt	8598	9494668	2010
11	Container	-Container	0–999	TEU	5397	8914568	1992
12	Container	-Container	1000–1999	TEU	11200	9395070	2007
13	Container	-Container	2000–2999	TEU	21560	9241475	2003
14	Container	-Container	3000–4999	TEU	36515	9238806	2003

15	Container	-Container	5000–7999	TEU	54942	9300465	2007
16	Container	-Container	8000–11999	TEU	58100	9486087	2015
17	Container	-Container	12000–14499	TEU	54200	9627980	2013
18.1	Container	-Container	14500-19999	TEU	59360	9619983	2014
18.2	Container	-Container	20000+	TEU	60380	9863302	2020
19	General cargo	-General Cargo	0–4999	dwt	882	8870384	1978
20	General cargo	-General Cargo	5000–9999	dwt	2648	9318670	2004
21.1	General cargo	-General Cargo	10000-19999	dwt	4413	7801312	1978
21.2	General cargo	-General Cargo	20000+	dwt	7980	9416719	2009
22	Liquefied gas tanker	-Liquefied Gas	0–49999	cbm	2869	9128661	1995
23.1	Liquefied gas tanker	-Liquefied Gas	50000-99999	cbm	12450	9604392	2013
23.2	Liquefied gas tanker	-Liquefied Gas	100000-199999	cbm	28687	9183269	2000
24	Liquefied gas tanker	-Liquefied Gas	200000+	cbm	37320	9397339	2009
25	Oil tanker	-Oil	0–4999	dwt	956	8810982	1988
26	Oil tanker	-Oil	5000–9999	dwt	2574	9539676	2009
27	Oil tanker	-Oil	10000–19999	dwt	4320	9046071	1993
28	Oil tanker	-Oil	20000–59999	dwt	8580	9248801	2003
29	Oil tanker	-Oil	60000–79999	dwt	11390	9414838	2010
30	Oil tanker	-Oil	80000–119999	dwt	13548	9290309	2004
31	Oil tanker	-Oil	120000–199999	dwt	17098	9224271	2002
32	Oil tanker	-Oil	200000+	dwt	26000	9681211	2015
33.1	Other liquids	-Other Liquids	0-999	dwt	306	9393838	2006
33.2	Other liquids	-Other Liquids	1000+	dwt	1765	9288306	2003
34.1	Ferry-pax only	---Passenger Ship	0-299	GT	1052	8612562	1986
34.2	Ferry-pax only	---Passenger Ship	300-999	GT	2043	9628075	2011
34.3	Ferry-pax only	---Passenger Ship	1000-1999	GT	2206	7315569	1973
35	Ferry-pax only	---Passenger Ship	2000+	GT	3200	9032159	1994

36	Cruise	---Passenger (Cruise) Ship	0-1999	GT	660	9086863	1994
37	Cruise	---Passenger (Cruise) Ship	2000-9999	GT	3440	9822516	2019
38	Cruise	---Passenger (Cruise) Ship	10000-59999	GT	18596	9210220	2001
39	Cruise	---Passenger (Cruise) Ship	60000-99999	GT	55216	9188037	2000
40.1	Cruise	---Passenger (Cruise) Ship	100000-149999	GT	67200	9424883	2010
40.2	Cruise	---Passenger (Cruise) Ship	150000+	GT	75624	9349681	2008
41	Ferry-RoPax	-Passenger/Ro-Ro Cargo	0-1999	GT	1118	9771561	2016
42.1	Ferry-RoPax	-Passenger/Ro-Ro Cargo	2000-4999	GT	3450	8404812	1985
42.2	Ferry-RoPax	-Passenger/Ro-Ro Cargo	5000-9999	GT	8312	8822222	1989
42.3	Ferry-RoPax	-Passenger/Ro-Ro Cargo	10000-19999	GT	13440	9275218	2005
42.4	Ferry-RoPax	-Passenger/Ro-Ro Cargo	20000+	GT	23820	9066772	1994
43	Refrigerated bulk	-Refrigerated Cargo	0-1999	dwt	852	8842533	1991
43.2	Refrigerated bulk	-Refrigerated Cargo	2000-5999	dwt	2978	8815023	1989
43.3	Refrigerated bulk	-Refrigerated Cargo	6000-9999	dwt	5296	9078452	1993
43.4	Refrigerated bulk	-Refrigerated Cargo	10000+	dwt	11475	9143099	1996
44	Ro-Ro	---Ro-Ro Cargo Ship AND ---Container/Ro-Ro Cargo Ship	0-4999	dwt	2516	8320640	1984
45.1	Ro-Ro	---Ro-Ro Cargo Ship AND ---Container/Ro-Ro Cargo Ship	5000-9999	dwt	9840	9183984	2000
45.2	Ro-Ro	---Ro-Ro Cargo Ship AND ---Container/Ro-Ro Cargo Ship	10000-14999	dwt	16290	8807416	1990
45.3	Ro-Ro	---Ro-Ro Cargo Ship AND ---Container/Ro-Ro Cargo Ship	15000+	dwt	19040	9437921	2010
46.1	Vehicle	---Vehicles Carrier	0-29999	GT	5980	9136967	1996
46.2	Vehicle	---Vehicles Carrier	30000-49999	GT	11560	9372327	2007
47.1	Vehicle	---Vehicles Carrier	50000+	GT	14280	9332547	2007
A	Ro-Ro Cargo Ship	---Ro-Ro Cargo Ship AND ---Container/Ro-Ro Cargo Ship	5000+	dwt	20070	Confidential	2003

B	Ro-Ro Cargo Ship	---Ro-Ro Cargo Ship AND ---Container/Ro-Ro Cargo Ship	5000--+	dwt	20070	Confidential	2004
C	Passenger/Ro-Ro Ship (Vehicles)	-Passenger/Ro-Ro Cargo	5000-9999	GT	25200	Confidential	2010
D	Passenger/Ro-Ro Ship (Vehicles)	-Passenger/Ro-Ro Cargo	2000-4999	GT	6120	Confidential	1997
E	Passenger/Ro-Ro Ship (Vehicles/Rail)	-Passenger/Ro-Ro Cargo	2000-4999	GT	6000	Confidential	1991
F	Passenger/Ro-Ro Ship (Vehicles/Rail)	-Passenger/Ro-Ro Cargo	2000-4999	GT	6000	Confidential	1992
G	Passenger/Ro-Ro Ship (Vehicles)	-Passenger/Ro-Ro Cargo	5000-9999	GT	24000	Confidential	2001
H	Passenger/Ro-Ro Ship (Vehicles)	-Passenger/Ro-Ro Cargo	5000-9999	GT	25920	Confidential	2003
I	Passenger/Ro-Ro Ship (Vehicles)	-Passenger/Ro-Ro Cargo	2000-4999	GT	7920	Confidential	1990

Supplementary Materials: US Naval Ships' Technical Manual fouling rating

US Naval Ships' Technical Manual fouling rating, fr_{NSTM} (Naval Sea Systems Command, 2006; Oliveira and Granhag, 2020)

fr_{NSTM} [-]	Type	Hull fouling condition
0	undetectable	Foul-free surface.
10	soft	Incipient slime, visible underlying paint/metal surface.
20	soft	Advanced slime, obscured underlying paint/metal surface. Juvenile barnacles ≤ 1 mm (Oliveira and Granhag, 2020).
30	soft	Soft fouling (e.g. filaments) < 76 mm in length and < 6.4 mm in height.
40	hard	Tubeworms < 6.4 mm in height. Encrusting bryozoans (Oliveira and Granhag, 2020).
50	hard	Barnacles < 6.4 mm in height.
60	hard	Combination of tubeworms and barnacles < 6.4 mm in height.
70	hard	Combination of tubeworms and barnacles > 6.4 mm in height.
80	hard	Tubeworms closely packed and upright from surface, or barnacles on top of each other, < 6.4 mm in height.
90	hard	Densely packed tubeworms or barnacles, > 6.4 mm in height; presence of mussels or oysters; or slime/grass overlay.
100	composite	All forms of fouling; soft animal fouling (tunicates) growing on various forms of hard fouling

Supplementary Materials: calculation of areal-averaged fouling rating

Mean fouling rating is defined for each visually inspected panel as:

$$\text{mean}(fr_{NSTM}) = \sum_{i=1}^N \frac{fr_{NSTM,i} \times \%cover_i}{100}$$

Equation 1

where N is the total number of different fouling ratings observed on a given panel, $fr_{NSTM,i}$ is the i^{th} fouling rating observed on that panel, and $\%cover_i$ is the percentage cover for that i^{th} fouling rating, evaluated using standard extent diagrams (ASTM D6990-05, 2005). As an example, a panel covered in half of its area by small barnacles ($fr_{NSTM,1} = 50$, $\%cover_1 = 50\%$) and otherwise covered by incipient/light slime ($fr_{NSTM,2} = 10$, $\%cover_2 = 50\%$) would have a $\text{mean}(fr_{NSTM})$ rating of 30.

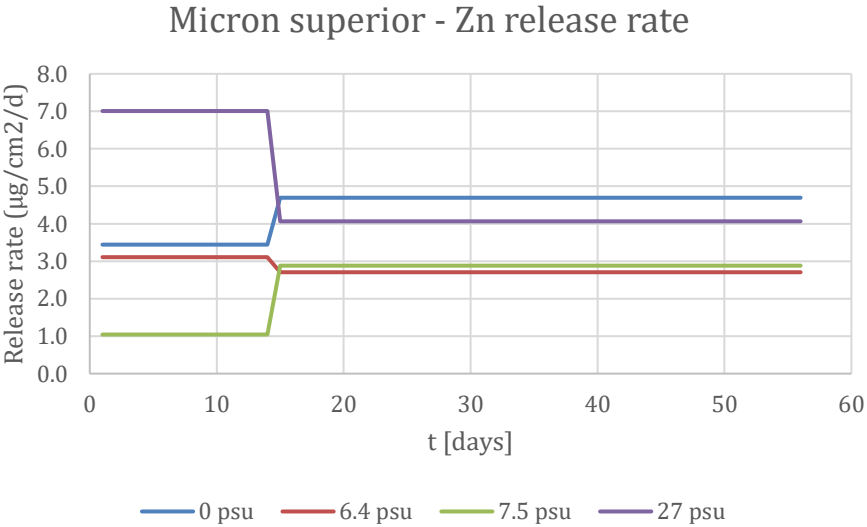
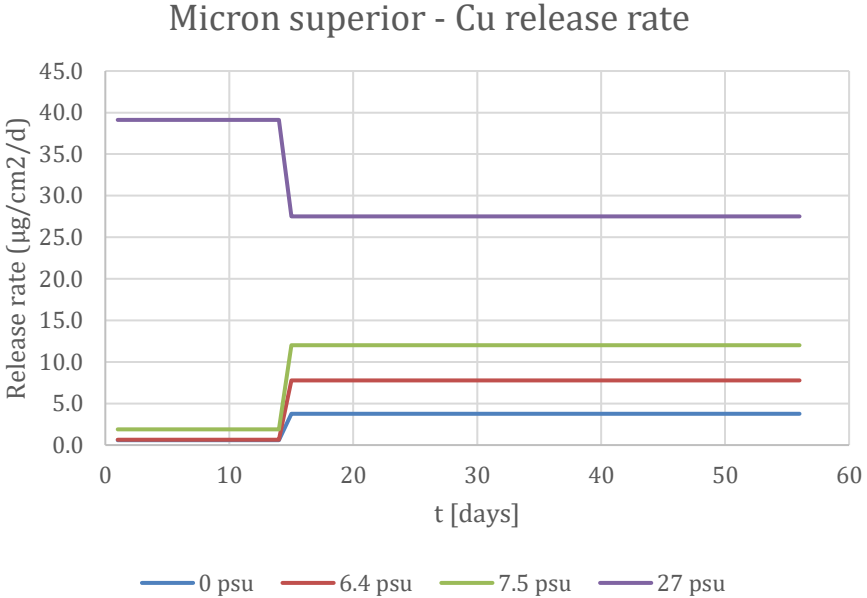
Supplementary Materials: Initial coating roughness conditions

Assumed values in HullMASTER for initial hull conditions and hydraulic equivalent sand grain roughness height k_s , which are converted from power or frictional penalties given in cited sources, using the method detailed in Oliveira et al. (2020), are as follows: (Abbreviations: IWHC = in-water hull cleaning)

Initial condition	k_s [μm], Lower bound	k_s [μm], Average	k_s [μm], Upper bound	Source, coatings and treatments
Full sandblasting: foul-release coating	0	15	30	Jotun Silicone: Seaquantum (Leer-Andersen, 2018) foul-release, normal application (Yeginbayeva and Atlar, 2018)
Full sandblasting: polishing antifouling and inert coating	30	40	60	Jotun: Antifouling Seaforce 60 (Leer-Andersen, 2018), linear polishing polymer, normal application (Yeginbayeva and Atlar, 2018)
Touch-up: foul- release coating	35	40	45	Foul-release, mimicked hull roughness (Yeginbayeva and Atlar, 2018)
Touch-up: polishing antifouling and inert coating	30	65	150	Jotun: Rough antifouling Seaforce 60, and flaked paint (Leer-Andersen, 2018), linear polishing polymer, mimicked hull roughness (Yeginbayeva and Atlar, 2018)
Proactive IWHC, negligible wear	same as out-docking	same as out-docking	same as out-docking	Currently assuming no coating deterioration.
Proactive IWHC, moderate wear	50	80	150	High pressure cleaning, best cleaning results (Leer-Andersen, 2018)
Reactive IWHC, high wear	70	150	300	Light cleaning, imperfect cleaning results (Leer-Andersen, 2018)

Supplementary Materials: release rate model

Passive release rates are modelled as a function of salinity, based on data from Lagerström et al. (2020), where the Cu and Zn release rates were measured between days 1-14 and 14-56 (elapsed time since coating immersion), and at 4 salinities (4 locations around Sweden), for a polishing copper antifouling coating (“Micron superior”, see coating details under Supplementary Materials: Reference biocidal coating), according to the following release rate charts:



Different equations thus apply for release rates at $t \leq 14$ days and at $t > 14$ days. However, as the data from Lagerström et al. (2020) is only for the average short-term release rate in the period 14-56 days, an assumption on the long-term release rate behavior of the paint was necessary, with a *Decrease ratio* applicable to the period $t > 14$ days, which is currently based on the release rate study by Valkirs et al. (2003) and assuming that the same decay ratio applies to both Cu and Zn:

Lower bound of 95%-confidence interval:

$$\begin{cases} RR_{Cu}(t) = 0.0715 * Salinity^2 - 0.6137 * Salinity - 0.1658, & t \leq 14 \text{ days} \\ RR_{Cu}(t) = (0.7078 * Salinity + 1.9919) * Decrease \text{ ratio}, & t > 14 \text{ days} \end{cases}$$

Equation 2

$$\begin{cases} RR_{Zn}(t) = 1.7, & t \leq 14 \text{ days} \\ RR_{Zn}(t) = 1.7 * Decrease \text{ ratio}, & t > 14 \text{ days} \end{cases}$$

Equation 3

Average value:

$$\begin{cases} RR_{Cu}(t) = 0.0662 * Salinity^2 - 0.3575 * Salinity + 0.5506, & t \leq 14 \text{ days} \\ RR_{Cu}(t) = (0.8836 * Salinity + 3.7304) * Decrease \text{ ratio}, & t > 14 \text{ days} \end{cases}$$

Equation 4

$$\begin{cases} RR_{Zn}(t) = 3.6, & t \leq 14 \text{ days} \\ RR_{Zn}(t) = 3.6 * Decrease \text{ ratio}, & t > 14 \text{ days} \end{cases}$$

Equation 5

Upper bound of 95%-confidence interval:

$$\begin{cases} RR_{Cu}(t) = 0.0608 * Salinity^2 - 0.1014 * Salinity + 1.267, & t \leq 14 \text{ days} \\ RR_{Cu}(t) = (1.0594 * Salinity + 5.4690) * Decrease \text{ ratio}, & t > 14 \text{ days} \end{cases}$$

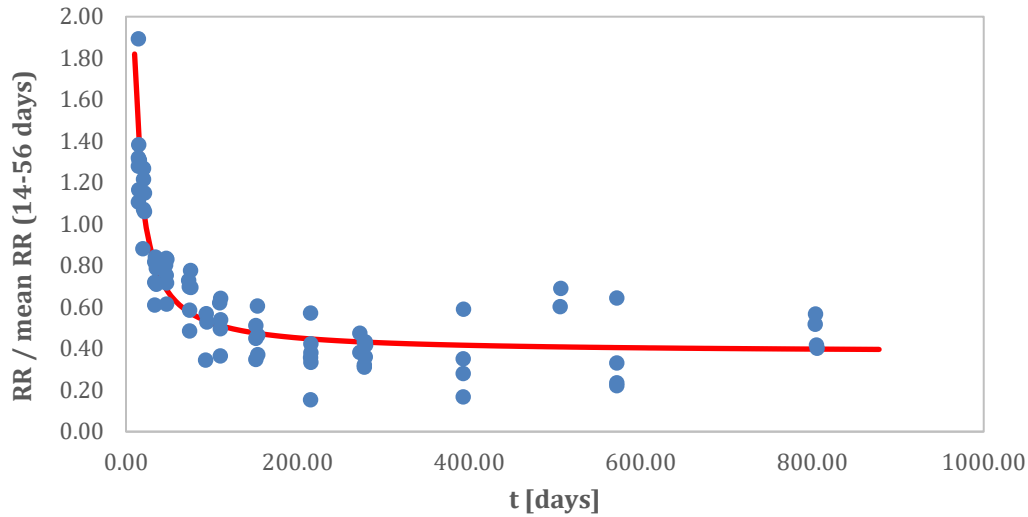
Equation 6

$$\begin{cases} RR_{Zn}(t) = 5.5, & t \leq 14 \text{ days} \\ RR_{Zn}(t) = 5.5 * Decrease \text{ ratio}, & t > 14 \text{ days} \end{cases}$$

Equation 7

where RR is release rate [$\mu\text{g}/\text{cm}^2/\text{day}$], t is time since last dry-docking [days], and *Decrease ratio* is the long-term change in release rate along time as obtained based from fitted curve to Valkirs et al. (2003) release rate data. This *Decrease ratio* is relative to the average release rate in the period 14-56 days from Lagerström et al. (2020) (see

above release rate charts), and defined based on curve fitting to data from Figure 6 in Valkirs et al. (2003) for 8 self-polishing coatings, as represented in the following release rate chart:



Curve fitting to the above data from to Valkirs et al. (2003) yields ($R^2 = 0.83$):

$$\text{Decrease ratio} = \frac{RR}{\text{mean RR (14 to 56 days)}} = 14.4/t + 0.38$$

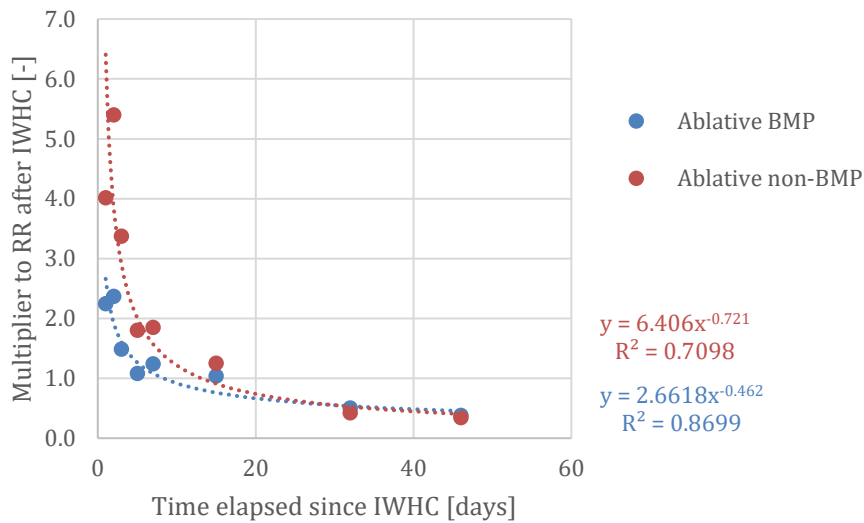
Equation 8

Finally, time steps for release rate are defined as 1/10 of the shortest idle or active vessel period, or a maximum 0.1 days, and *Salinity* during vessel transit is defined as average between two ports.

Besides passive release rates, a certain increased amount of antifouling compounds is released during and after in-water hull cleaning (IWHC), depending on the cleaning method. Currently, pulse emissions due to IWHC activities are modelled in HullMASTER assuming a certain coating wear, in $\mu\text{m}/\text{event}$, and the biocidal weight content per coating thickness removed, in $\mu\text{g}/\mu\text{m}/\text{cm}^2$, conservatively assumed as that of intact layers of coating (Tribou and Swain, 2017). For proactive cleaning, i.e. gentle and frequent cleaning of early forms of soft fouling, two levels of wear are considered: negligible wear, 0 $\mu\text{m}/\text{event}$ (Oliveira and Granhag, 2020) and moderate wear, 25 $\mu\text{m}/\text{event}$ (Morrisey et al., 2013, p. 93, ablative coatings and light brushing). For reactive cleaning, i.e. requiring aggressive methods to remove calcareous fouling, a higher wear of 75 $\mu\text{m}/\text{event}$ is assumed (Morrisey et al., 2013, p. 93, ablative coatings, hard brushing). The user may manually adjust the amount of wear according to available data and technology. Regarding effluent treatment, default biocide removal efficacy is

currently set to 0% (no treatment), due to scarcity of independent data (Scianni and Georgiades, 2019; Tamburri et al., 2020). Biocide release due to IWHC is added to passive release on the cleaning date, and increased passive release rates in period subsequent to a cleaning event are modelled according to Earley et al. (2014), as detailed next.

In case of in-water hull cleaning (IWHC) on antifouling copper coating type, increased release rates in period subsequent to a cleaning event are modelled according to Earley et al. (2014), using Best Management Practice (BMP) for moderate coating wear (proactive cleaning, moderate wear), or non-BMP for higher coating wear (reactive cleaning, high wear), according to the following fitted curves, which are used as multipliers to an underlying passive release rate (no changes applicable to proactive cleaning with negligible coating wear):



The datapoints plotted above are from Earley et al. 2014, fitted curves by the Authors of the current publication.

Supplementary Materials: Reference biocidal coating

Paint product: International® Micron Superior

Wet Film Thickness [μm] = 167

Dry Film Thickness [μm] = 100

t, lifetime of the coating [months] = 24

La, fraction active ingredient released [-] = 0.9

Paint density [kg/L] = 1.8

Volume of solids fraction [%] = 60

Wet weight Cu₂O fraction [% Cu₂O] = 31.94

Wet weight CuO fraction [% CuO] = 0

Wet weight other copper [% Cu] = 0

Wet weight ZnO fraction [% ZnO] = 9.96

Wet weight other zinc [% Zn] = 0

a, Cu in Cu₂O fraction [-] = 0.8882

a, Cu in CuO fraction [-] = 0.7989

a, Zn in ZnO fraction [-] = 0.8034

X(Cu), initial 14-days release [$\mu\text{g}/\text{cm}^2$] = 308.03

Y(Cu), steady state release [$\mu\text{g}/\text{cm}^2/\text{day}$] = 10.27

X(Zn), initial 14-days release [$\mu\text{g}/\text{cm}^2$] = 86.88

Y(Zn), steady state release [$\mu\text{g}/\text{cm}^2/\text{day}$] = 2.90

Supplementary Materials: validation of hull roughness penalties

In order to validate powering penalties, which are estimated in HullMASTER according to methods described in previous sections, hull-and-propeller performance is analyzed for 9 Ro-Ro vessels (Roll-on/Roll-off Cargo, as well as Roll-on/Roll-off + Passengers), that operate in the Baltic Sea region.

Vessel particulars are presented in Table 1 for the 9 vessels included in the current validation. These vessels operate in the Baltic Sea region and had their hulls coated, in most cases, with biocidal copper antifouling coatings (AF). Additionally, a few vessels have been lately experimenting with alternative coatings, including: an inert abrasion-resistant coating (Inert ARC: vessel A), a hybrid silicone coating containing a booster biocide (FR-Hybrid, 5-10% copper pyrithione: vessels B and H), a self-polishing copper-free coating containing a booster biocide (Cu-free SPC, 5-10% zinc pyrithione: vessel C), and a pure foul-release silicone coating (FR-Pure: vessel I). Selected vessels have features in common, such as ship type (Ro-Ro cargo vessels, i.e. Roll-on/Roll-off, and Ro-Ro with passengers or Ro-Pax vessels, i.e. Roll-on/Roll-off + Passengers), but they differ in terms of size category (deadweight tonnage in range 2,500-11,000 dwt or gross tonnage 10,000-58,000 GT), as well as in terms of vessel age, in range 5-28 years, with average 17 years of age at start of data collection. Dry-docking intervals are in the range of ~2-3 years, whereas vessel activity, i.e. share of time at vessel speed >1 knot, varies in a range 30-70%. The total amount of available data for validation corresponds to nearly 40 vessel-years (Table 1, length of data).

Onboard-collected variables, sampling rate and the sources for baseline performance curve are listed in Table 2 for all studied vessels.

Vessels A, B and C are operated by the same company, where A and B are sister vessels operating between Kattegat Sea and North Sea, and C operates between Baltic Proper and Danish Straits. These vessels have the most comprehensive set of in-service performance data, available as 10-min average and standard-error values for each of vessel speed, shaft power (and/or fuel consumption), weather (wind speed, wind direction, and significant wave height), rudder angle, sea depth, and vessel loading conditions (draft and trim). However, speed through water STW has been proven unreliable for vessels A and B and unavailable for vessel C, so speed over ground SOG is currently used as a proxy, even though this includes errors associated with sea currents (Oliveira et al., 2020). Also, vessel C was not equipped with a torque meter for determining shaft power, so propulsion power is estimated using volumetric fuel consumption, assuming fuel oil density of 0.9 t/m³ and reference specific fuel oil consumption ($SFOC = 175 \text{ g/kWh @ 80\% of MCR for a Wärsilä 12V46F engine}$).

Table 1 – Vessel particulars of 9 vessels included in model validation. Legend: Ro-Ro – Roll-on/Roll-off ship, AF – conventional biocidal antifouling coating, ARC – abrasion-resistant coating, FR – foul-release coating, SPC – polishing coating, MCR – Maximum Continuous Rating for propulsion, L_{pp} – length between perpendiculars, B – breadth, T_{design} – design draft, ∇ – displacement, C_B – block coefficient, DD – dry-docking.

Vessel	Ship type	Hull coatings	Service speed [knots]	MCR [kW]	L_{pp} [m]	B [m]	T_{design} [m]	∇ [m ³]	C_B [-]	DD interval [years]	Activity [%]	Age at start of data [years]	Length of data [years]
A	Ro-Ro Cargo Ship	AF Inert ARC	22.50	20070	189.690	26.500	7.350	20000	0.54	2.0	64	11	5.2
B	Ro-Ro Cargo Ship	AF FR- Hybrid	22.50	20070	189.690	26.500	7.350	20000	0.54	2.0	63	10	5.3
C	Passenger/Ro-Ro Ship (Vehicles)	AF Cu-free SPC	24.00	25200	176.920	26.600	6.400	18325	0.61	2.8	69	5	4.5
D	Passenger/Ro-Ro Ship (Vehicles)	AF	13.00	6120	102.220	27.600	5.500	6600	0.43	2.0	30	22	1.5
E	Passenger/Ro-Ro Ship (Vehicles/Rail)	AF	13.50	6000	94.830	27.600	5.500	7994	0.56	2.0	57	28	1.8
F	Passenger/Ro-Ro Ship (Vehicles/Rail)	AF	13.50	6000	94.900	27.600	5.700	-	-	2.0	55	26	2.3
G	Passenger/Ro-Ro Ship (Vehicles)	AF	22.00	24000	223.110	28.700	6.300	21250	0.53	3.0	59	16	3.5
H	Passenger/Ro-Ro Ship (Vehicles)	AF FR- Hybrid	22.00	25920	226.450	29.300	6.314	31409	0.75	3.0	58	14	3.5
I	Passenger/Ro-Ro Ship (Vehicles)	FR-Pure	16.00	7920	142.420	24.000	5.920	13647	0.67	1.9	54	17	12

Table 2 – Onboard-collected variables, sampling rate, and source for baseline performance curves. Legend: + variable available and included in the analysis, (+) variable available but excluded from analysis, SOG – speed over ground, STW – speed through water, Other – estimated from sources external to the vessel, Azimuth – thruster azimuth angle used instead of rudder angle, P – shaft power, FC – fuel consumption, BF – Beaufort scale, A±SE – average ± standard error.

Vessel	Area	SOG [knots]	STW [knots]	P [kW]	FC [kg/h]	FC [L/h]	Wind speed [m/s] direction [°]	Wind force [BF]	Rudder angle [°]	Sea depth [m]	Draft [m]	Trim [m]	Sampling rate	Baseline power-speed curve
A	Kattegat Sea and North Sea	+	(+)	+		(+)	+		+	+	+	+	10-min A±SE	Model test
B	Kattegat Sea and North Sea	+	(+)	+		(+)	+		+	+	+	+	10-min A±SE	Model test
C	Baltic Proper	+				+	+		+	+	+	+	10-min A±SE	Sea trial
D	Danish Straits	+	Other	+		(+)	Other						Every 15 s	Sea trial
E	Danish Straits	+	Other	+		(+)	Other		Azimuth				Every 15 s	Model+Sea trial
F	Danish Straits	+	Other	+		(+)	Other		Azimuth				Every 15 s	Model+Sea trial
G	Kattegat Sea and Danish Straits	(+)	+	+		(+)	+			+		+	Every minute	Model test
H	Kattegat Sea and Danish Straits	(+)	+	+		(+)	+			+		+	Every minute	Empirical
I	Baltic Proper	+			+			+			+		Sea passage (2 times/day)	Empirical

Further, while vessels A and B (sister vessels) had available model test results for baseline performance at 16 speed values, 4 draft values and 6 trim values (Oliveira et al., 2020), vessel C had only a sea trial report, at 1 loading condition (draft and trim) and 5 speed values. Consequently, data from vessel C is filtered for vessel displacement within 5% of the sea trial displacement value (in metric tons), and vessel speed is further corrected using the Admiralty formula (ISO, 2016) and filtered to the speed range from the sea trial (speed trial).

Vessels D, E and F all operate the same route between two ports in the Danish Straits. These vessels are double-ended ferries equipped with 4 propellers. In vessel D, propellers are shaft-driven, whereas vessels E and F (sister ships) are equipped with azimuthal thrusters. Data was collected at a rate of 1 datapoint / second (data snapshots), which were then resampled for convenient data processing at 0.07 Hz, or 1 datapoint every 15 seconds, according to standard method (ISO, 2016). No data on STW was recorded, so hindcast data for local sea currents is used instead, as provided by external sources (E.U. Copernicus Marine Service Information, 2020). Sea currents were thus sampled at the midpoint between the two ports of call, which are separated by a distance of only 2 nautical miles (~3.7 km), and this external hindcast data is used in filtering in-service performance data to sea current <0.5 knots. Considering the proximity of the two ports of call, missing weather data is also obtained externally, from a weather station located in one of the ports of call. No data was available on sea depth, draft or trim for these vessels. On this specific route, other methods, such as data validation, outlier detection and filtering procedures (described below), may cover for the lack of data on sea depth, where sea depth is expected to correlate with stable vessel speed, defined according to outlier detection (ISO, 2016). Also, vessels D, E and F operate at approximately constant loading conditions, according to the vessel operator, and draft and trim may thus be assumed constant. Finally, instead of rudder angle, azimuth angle of the thrusters is used to calculate the force component acting along vessel length and the force component acting sideways, according to manufacturer of data collection system:

$$P_{sideways} = \sum_{i=1}^4 |\sin \theta_i \times P_i|$$

Equation 9

where θ_i and P_i are the azimuth angle and delivered power to thruster i , respectively. A specific filter is thus applied to these vessels, using only datapoints with power sideways <5% of total power delivered by the azimuthal thrusters. Finally, vessel D had sea trial results as baseline performance, which had to be extrapolated to lower speeds using a fitted equation (generic power model $P = aV^b$ is used). Vessels E and F had model test results for one loading condition and 11 speed cases, as well sea trial results for only one loading condition and one speed. Due to the limited data from sea trial for

vessels E and F, sea trial results were only used for scaling higher-detail model test predictions to sea-trial speed performance.

Vessels G and H (**Error! Reference source not found.**) are Passenger/Ro-Ro ships operating the same route in Kattegat Sea and Danish Straits. Data was collected at a rate of 1 datapoint / minute (data snapshots). Both speed loggers and torque meters were installed onboard, enabling reliable STW and shaft power measurements, respectively. Weather and sea depth data was also measured onboard. However, no rudder angle or draft values were available. Whereas draft may be assumed approximately constant for these vessels, absence of rudder data may result in overestimation of powering penalties in some datapoints. However, validation and outlier detection for other variables may still filter out periods when vessels were maneuvering or changing course. Regarding baseline curves, while vessel G had model test results readily available (one vessel loading condition, five speed values), vessel H had no available baseline power-speed curves. For vessel H, an empirical approximate prediction method is used (Holtrop and Mennen, 1982), together with assumption of a 25% sea margin to MCR at service speed (Woud and Stapersma, 2016, p. 415).

Data acquisition on vessel I, which operates in the Baltic Proper, is described in more detail elsewhere (Kowalski, 2020) and the raw data was kindly shared by the author of that study. Data corresponds to sea-passage datapoints, typically with 2 sea passages per day, including fuel consumption (in kg), average speed over ground SOG calculated based on sea passage time (hours) and distance travelled (nautical miles), and Beaufort wind force (BF) representative for the entire duration of each sea passage. Performance results may therefore include confounding factors such as: varying engine performance, sea depth, instant speed, sea currents and rudder angle. Propulsive power consumption is estimated based on average fuel consumption (in kg/h), assuming an average specific fuel oil consumption $SFOC = 184$ g/kWh for a Sulzer/Wärtsilä 6ZA40S engine. For this vessel, no baseline power-speed performance curve was available. Therefore, an empirical approximate prediction method is also used also for this vessel (Holtrop and Mennen, 1982), together with assumption of a 25% sea margin to MCR at service speed (Woud and Stapersma, 2016, p. 415). Reported vessel speed is further corrected using the Admiralty formula (ISO, 2016), according to loading condition, based on reported draft for each sea passage.

Data validation and outlier detection is performed for vessels with data sampling rate higher than every 10 minutes (vessels D-H, **Error! Reference source not found.**), by removing datapoints with missing data and applying Chauvenet's criterion for outlier detection, as described elsewhere in more detail (ISO, 2016). After these validation steps, 10-min averages are used in calculating power-speed performance, as detailed next.

For the current validation purposes, percentage powering penalties P_{diff} are used in comparing HullMASTER predictions (**Error! Reference source not found.** and

REF_Ref55997812 \h **Error! Reference source not found.**) to the actual performance determined based on in-service performance data, where P_{diff} is defined as:

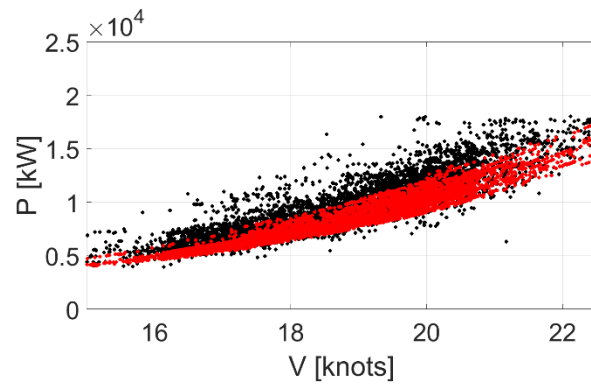
$$P_{diff}[\%] = \frac{P_{measured} - P_{baseline}}{P_{baseline}} \times 100 = \frac{\Delta P}{P_{baseline}} \times 100$$

Equation 10

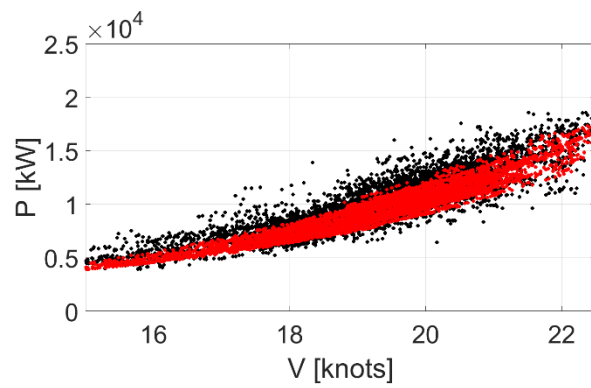
where $P_{measured}$ is the measured propulsion power (shaft power) and $P_{baseline}$ is the baseline calm-water propulsion power for a hydraulically smooth hull, both in kW. Measured power $P_{measured}$ is corrected for factors such as wind resistance, where raw in-service performance data is filtered for wind speed (≤ 7.9 m/s, or \leq Beaufort 4), sea depth and rudder angle (ISO, 2016), depending on data availability from each vessel (**Error! Reference source not found.**).

Precision uncertainty is estimated by calculating time average values together with 95% confidence intervals for data periods of 3 months, according to standard procedure (ISO, 2016). No estimates of bias uncertainty are currently available for the above methods (please refer to discussion in Oliveira et al., 2020).

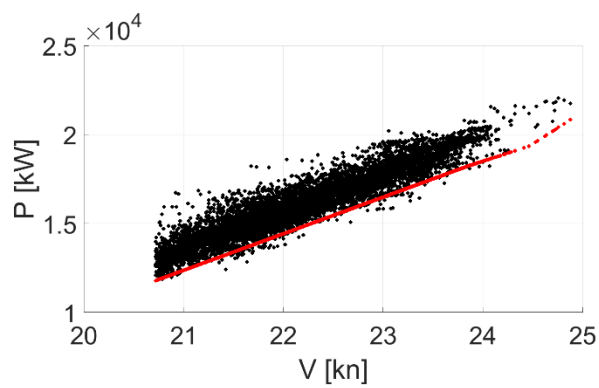
Supplementary Materials: onboard-measured power $P_{measured}$ and baseline power $P_{baseline}$



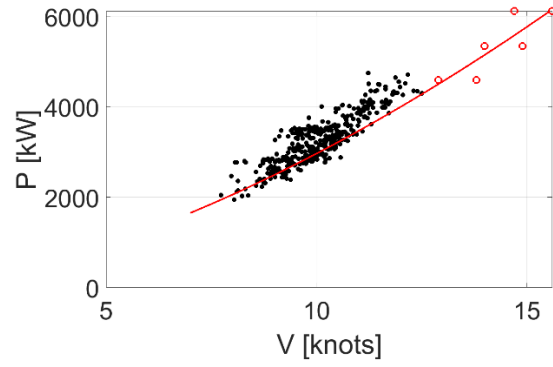
Vessel A: Filtered data, **Baseline**



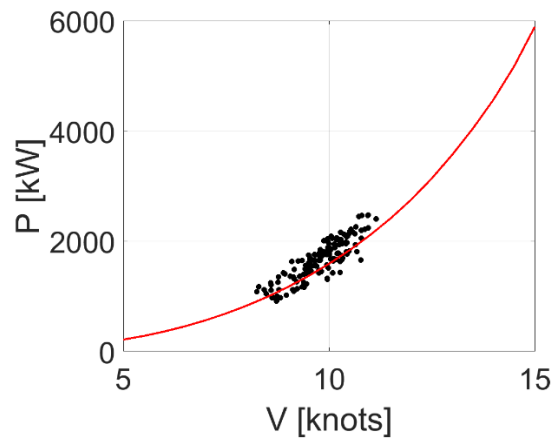
Vessel B: Filtered data, **Baseline**



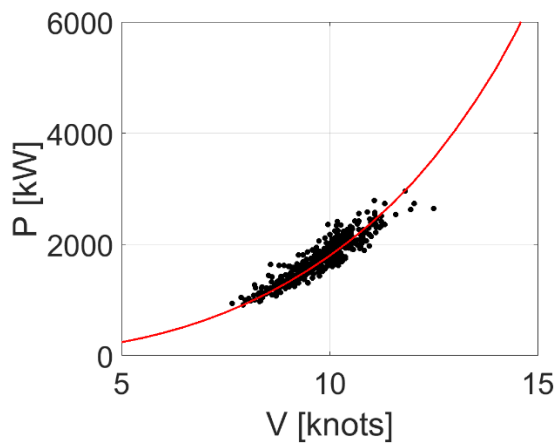
Vessel C: Filtered data, **Baseline**



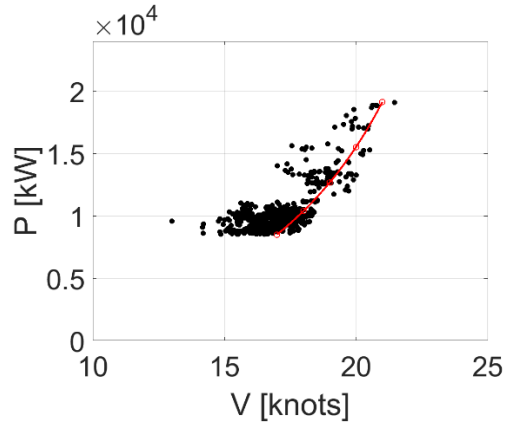
Vessel D: Filtered data, **Baseline**



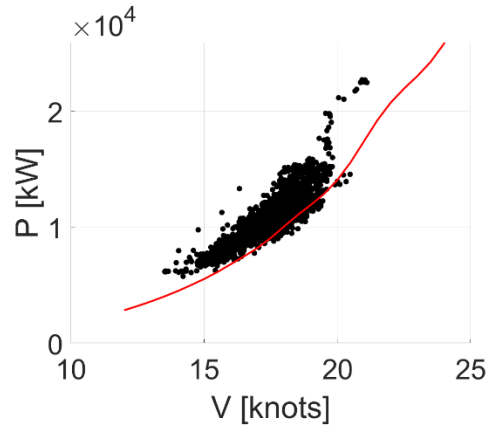
Vessel E: Filtered data, **Baseline**



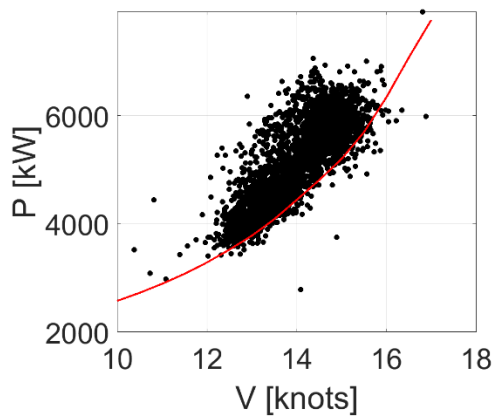
Vessel F: Filtered data, **Baseline**



Vessel G: Filtered data, **Baseline**



Vessel H: Filtered data, **Baseline**



Vessel I (data from Kowalski, 2020): Filtered data, **Baseline**

Supplementary Materials: Emission Factors

Emissions to air and water due to hull roughness are divided into the following themes: climate change (CO₂-equivalent emissions), health impact (NO_x, SO_x, PM_{2.5}, and NMVOC), marine eutrophication (N deposition), and marine ecotoxicity due to increased scrubber effluent as a result of hull roughness penalties (**Error! Reference source not found.**).

Emissions are grouped under those calculated using energy-based emission factors [kg/kWh], and those calculated using fuel-based emission factors [kg/kg of fuel]. A detailed description of assumed emission factors, based on the 4th IMO GHG study (IMO, 2020) is given in the *Supplementary Materials: Emission Factors*.

Fuel-based factors require further details on main engine's specific fuel consumption (SFC) [g fuel / kWh], given as a function of engine load [kW or % of engine MCR]. SFC curves are estimated for a given vessel based on reference values (IMO, 2020, Table 19), and converted to total fuel consumption, as described in *Supplementary Materials: specific and total fuel consumption*.

Finally, the user may also select to propel a vessel on battery power (fully electric propulsion). Upstream emissions are however not currently accounted for, following a tank(battery)-to-propeller approach.

Climate change-related emissions are first estimated for each species, including CO₂, CO, CH₄, N₂O, and black carbon (BC). Emission factors are obtained directly from the 4th IMO GHG study (IMO, 2020), implemented as fuel-based emissions factors for CO₂ and BC (in the case of BC, all fuels except Liquefied Natural Gas, LNG), whereas energy-based emission factors are used for CH₄, CO, N₂O, and BC (in the case of BC, only for LNG). It should be noted that for BC, emission factors carry comparatively larger uncertainties, and emission factors are simplistically assumed to depend on engine load, through an engine load multiplier and a load exponent (IMO, 2020, pp. 95–96). Being load-dependent, emission factors for BC are therefore calculated and implemented directly at the level of propulsive power time series, rather than simply multiplying emission factors (kg/kg fuel or kg/kWh) by the final sums of fuel or energy penalties, as is the case for nearly all other emission factors (except particulate matter, described further below in this section). Emission factors for greenhouse species, which depend on fuel type (for all species), engine speed (all except CO₂ and BC), engine stroke (only applicable for BC) and type of LNG engine (all except CO₂), are further normalized to equivalent CO₂ emissions, CO₂e. The latter is implemented using 100-year greenhouse warming potential, or 100-y GWP, which corresponds to tons of CO₂e per ton of a given species (IMO, 2020): GWP(CO₂) = 1, GWP(CO) = 1, GWP(CH₄) = 28, GWP(N₂O) = 265, GWP(BC) = 900.

For health impact of fuel penalties, energy-based emission factors (g / kWh) are used for NO_x, particulate matter PM_{2.5} and non-methane volatile organic compounds

NMVOC emissions, whereas SO_x emissions are modelled using fuel-based emission factors (g / g of fuel). Again, following assumptions and methodology used in IMO 4th GHG study (IMO, 2020), health-related emission factors depend on fuel type (for all species), sulfur content (SO_x and PM_{2.5}), engine-built year (NO_x), engine speed (NO_x and NMVOC), and LNG engine type (all species). PM_{2.5} emission factors are estimated based on the assumption that these emissions correspond to 92% mass fraction of a wider particle-size range, PM₁₀ (IMO, 2020, p. 94). Finally, the final sum of emissions of all these substances are calculated by multiplying each emission factor by estimates of total fuel (or energy) consumption penalty, except for PM_{2.5} emissions, which are dependent on engine load. In the latter case, emission factors for PM_{2.5} are calculated and implemented directly at the level of propulsive power time series, similarly to BC (please see above in this section, under climate change impact). Exhaust after-treatment techniques are also included in HullMASTER, based on previously published assumed efficacies of NO_x reduction and exhaust scrubbing techniques (Jalkanen et al., 2009). Specifically, a default exhaust scrubber efficacy of 95% is implemented, applicable when a high-sulfur content fuel is selected (>0.1% S), directly reducing emission factors for SO_x and PM_{2.5} by 95% (Jalkanen et al., 2009).

Using the estimates for NO_x emissions above, impact on marine eutrophication is estimated based on an 18% deposition of emitted nitrogen in a given sea basin (Ytreberg et al., 2021). The latter emitted nitrogen is simply calculated as fraction of nitrogen (N) contained in NO_x, i.e. $0.3035 \times$ emission factor, where 0.3035 is the mass fraction of N in NO₂. These emissions are further modified to take into account the percentage of time a ship is travelling in Baltic Proper, Gulf of Finland and Gulf of Riga (user input: % of active time in these sub-basins), assuming that nitrogen is deposited in the same sea basin as NO_x is emitted, and that N contributes to marine eutrophication in the Baltic Sea only when emitted and deposited in these sub-basins (Ytreberg et al., 2021).

Emission factors are also implemented for increased scrubber emissions due to propulsive power penalties (caused by hull roughness) in scrubber-fitted vessels, which has an impact in terms of marine ecotoxicity. For open-loop seawater scrubbers, an emission factor of 72-108 m³ of scrubber water / MWh is assumed, with an average of 90 m³ / MWh (Ytreberg et al., 2021). Lower values of 0.20-0.68 m³/MWh are assumed for closed-loop freshwater scrubbers, with an average of 0.44 m³ / MWh (Ytreberg et al., 2021). The environmental valuation of these emissions, in €/m³, is further addressed in section **Error! Reference source not found.** of the paper (**Error! Reference source not found.**).

Following an average-speed modelling approach, only those air and scrubber emissions that occur while the vessel is assumed to be cruising at an average speed are included in the analysis, thus excluding emissions in port, anchorage, or

maneuvering. Also, a tank-to-propeller approach is followed, so that upstream well-to-tank emissions (embedded emissions) are not currently included.

Supplementary Materials: Specific and total fuel consumption

Specific fuel consumption (SFC) curves are obtained as a function of fuel type (LNG or Heavy Fuel Oil, HFO), engine type (only when running on LNG), engine-built year, and engine speed (in rpm). This baseline SFC curve is then converted to specific consumption of a given selected fuel, by further taking into account energy density, i.e. the lower calorific value LCV of selected fuel, in MJ / kg (IMO, 2020, p. 88). The total fuel consumption penalty due to hull roughness is calculated as:

$$Fuel\ penalty\ [kg] = \sum_{i=1}^N [P_{rough,i} \times SFC(P_{rough,i}) - P_{smooth,i} \times SFC(P_{smooth,i})] \times \Delta t_i$$

Equation 11

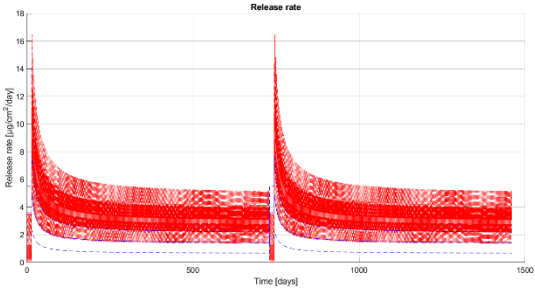
where N is the total number of voyages, $P_{rough,i}$ and $P_{smooth,i}$ are the calm-water power consumption values on the i^{th} voyage (in kW), respectively for the rough and smooth hull conditions, SFC is the specific fuel consumption for user-selected fuel (in kg/kWh), which is a function of engine load (i.e. P_{rough} or P_{smooth}) according to formula used in IMO 4th GHG study (IMO, 2020, p. 89), and Δt_i is the duration of the i^{th} voyage (in hours).

Supplementary Materials: Characterization factors and damage costs

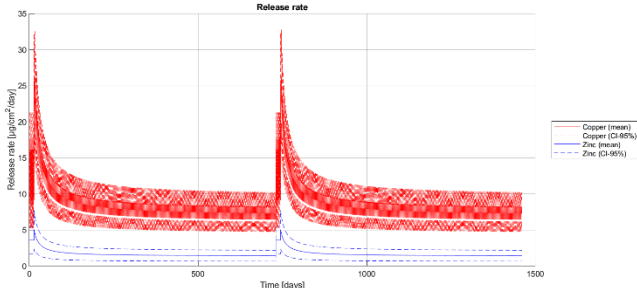
Characterization factors and damage costs for marine ecotoxicity. Lower and upper bounds correspond to 95% confidence intervals.

Substance or waste stream	Value	Units	Reference
Characterization factors			
Copper, Cu	1572.79	kg 1,4-DCB eq. / kg Cu	(Ytreberg et al., 2021)
Zinc, Zn	342.33	kg 1,4-DCB eq. / kg Zn	
Scrubber water, open loop	Lower = 0.11 Mean = 0.23 Upper = 0.35	kg 1,4-DCB eq. / m ³	
Scrubber water, closed loop	Lower = 3.3 Mean = 7.8 Upper = 12.3	kg 1,4-DCB eq. / m ³	
Damage costs			
1,4-Dichlorobenzene	Lower = 0.86 Mean = 1.26 Upper = 1.52	€ ₂₀₂₀ / kg emission	(Noring et al., 2016; Ytreberg et al., 2021)
Copper, Cu	Lower = 1352 Mean = 1986 Upper = 2388	€ ₂₀₂₀ / kg emission	Based on the above data, and assuming a 3% inflation rate (Schultz et al., 2011)
Zinc, Zn	Lower = 294 Mean = 433 Upper = 520	€ ₂₀₂₀ / kg emission	
Scrubber water, open loop	Lower = 0.09 Mean = 0.29 Upper = 0.53	€ ₂₀₂₀ / m ³ emission	
Scrubber water, closed loop	Lower = 2.84 Mean = 9.85 Upper = 18.68	€ ₂₀₂₀ / m ³ emission	

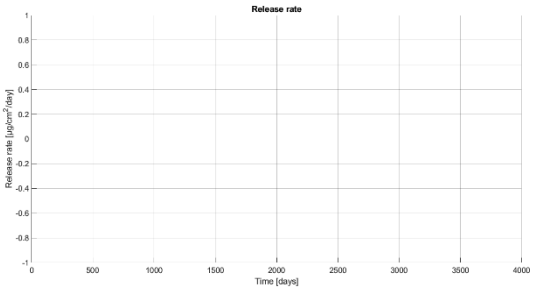
Supplementary Materials: Intermediate results



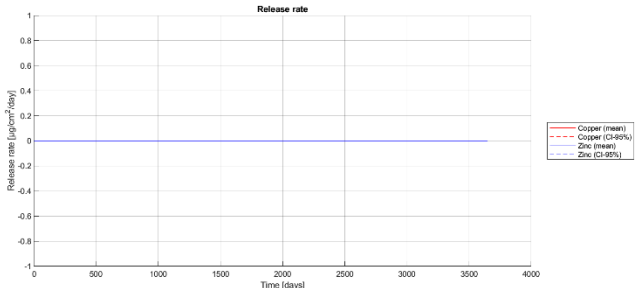
a1) Baltic Proper, Scenario 0



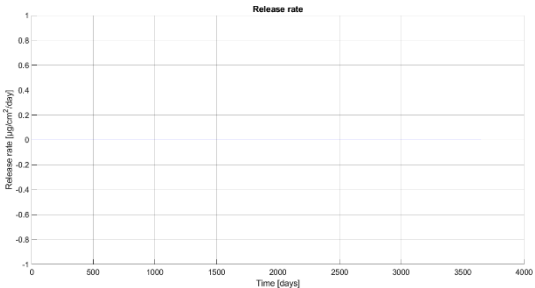
a2) Baltic Transition, Scenario 0



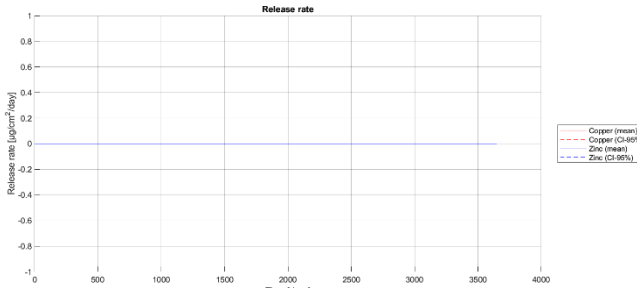
b1) Baltic Proper, Scenario 1



b2) Baltic Transition, Scenario 1

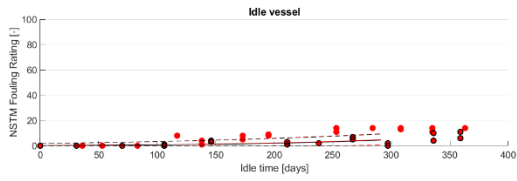


c1) Baltic Proper, Scenario 2

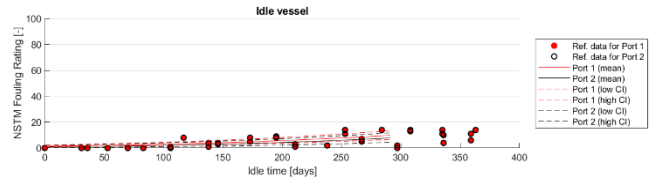


c2) Baltic Transition, Scenario 2

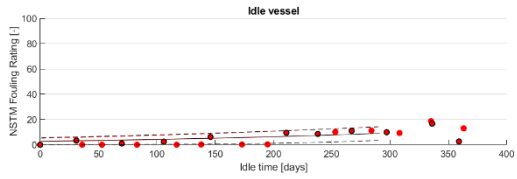
Figure 1 – Biocide release rates. Scenario 0 – Antifouling biocidal coating, Scenario 1 – Foul-release coating, Scenario 2 – Inert abrasion-resistant coating.



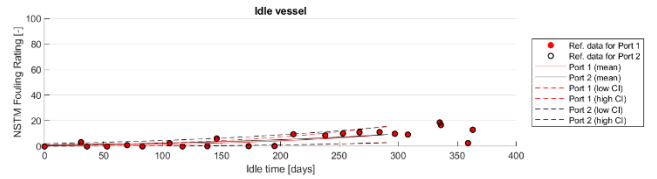
a1) Baltic Proper, Scenario 0



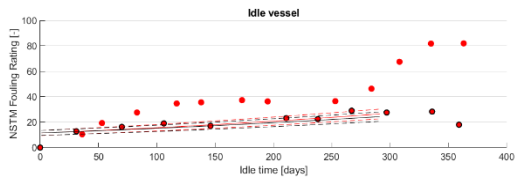
a2) Baltic Transition, Scenario 0



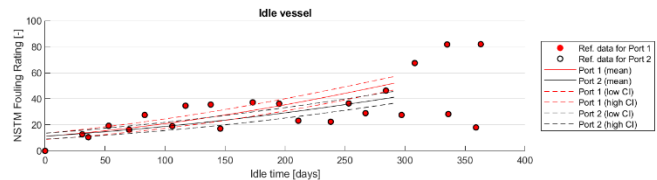
b1) Baltic Proper, Scenario 1



b2) Baltic Transition, Scenario 1

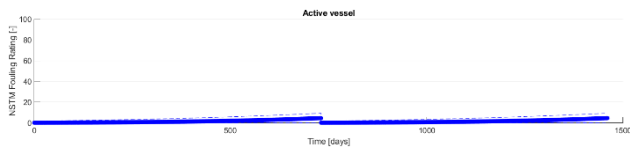


c1) Baltic Proper, Scenario 2

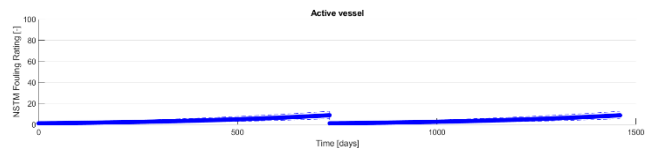


c2) Baltic Transition, Scenario 2

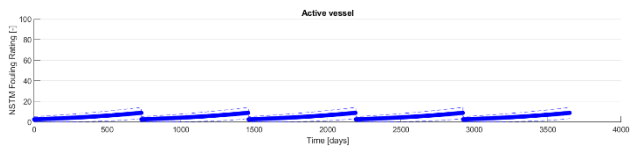
Figure 2 – Fouling growth on idle vessel. Scenario 0 – Antifouling biocidal coating, Scenario 1 – Foul-release coating, Scenario 2 – Inert abrasion-resistant coating.



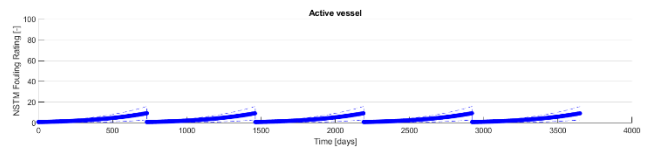
a1) Baltic Proper, Scenario 0



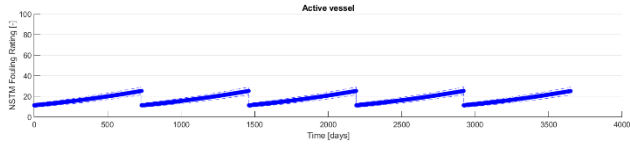
a2) Baltic Transition, Scenario 0



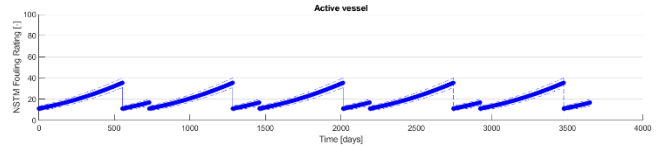
b1) Baltic Proper, Scenario 1



b2) Baltic Transition, Scenario 1

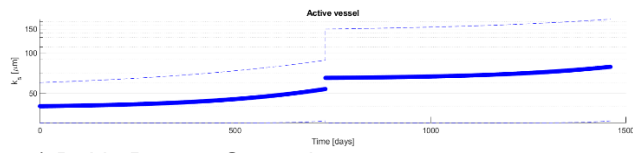


c1) Baltic Proper, Scenario 2

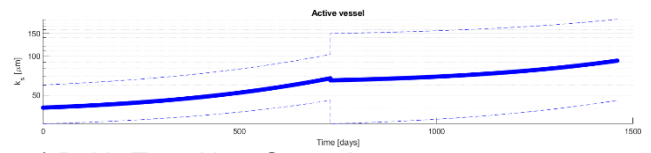


c2) Baltic Transition, Scenario 2

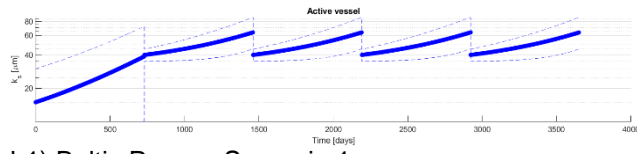
Figure 3 – Fouling growth on active vessel. Scenario 0 – Antifouling biocidal coating, Scenario 1 – Foul-release coating, Scenario 2 – Inert abrasion-resistant coating.



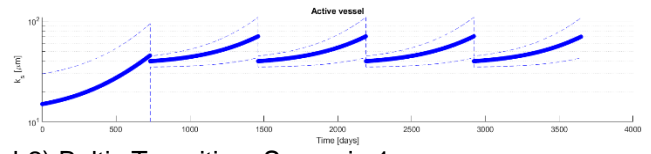
a1) Baltic Proper, Scenario 0



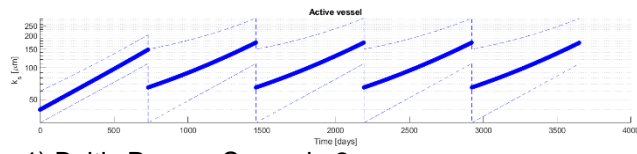
a2) Baltic Transition, Scenario 0



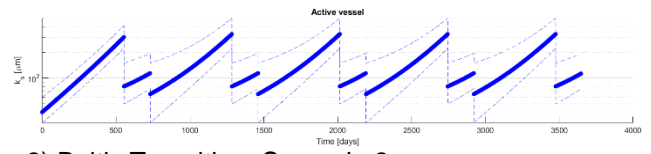
b1) Baltic Proper, Scenario 1



b2) Baltic Transition, Scenario 1

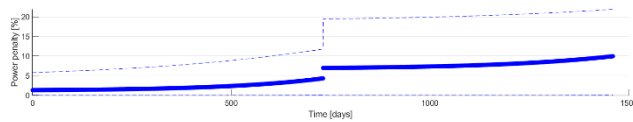


c1) Baltic Proper, Scenario 2

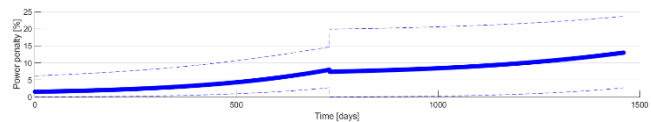


c2) Baltic Transition, Scenario 2

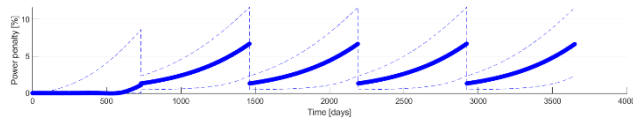
Figure 4 – Modelled hull roughness, k_s . Scenario 0 – Antifouling biocidal coating, Scenario 1 – Foul-release coating, Scenario 2 – Inert abrasion-resistant coating.



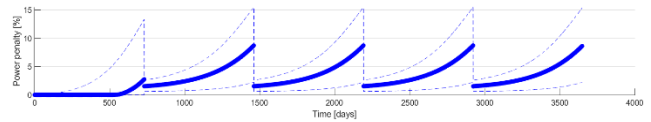
a1) Baltic Proper, Scenario 0



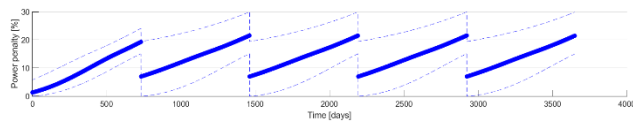
a2) Baltic Transition, Scenario 0



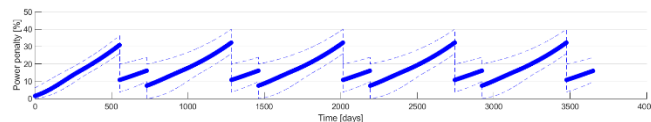
b1) Baltic Proper, Scenario 1



b2) Baltic Transition, Scenario 1



c1) Baltic Proper, Scenario 2



c2) Baltic Transition, Scenario 2

Figure 5 – Percentage powering penalty on active vessel. Scenario 0 – Antifouling biocidal coating, Scenario 1 – Foul-release coating, Scenario 2 – Inert abrasion-resistant coating.

References

- ASTM D6990-05, 2005. Standard Practice for Evaluating Biofouling Resistance and Physical Performance of Marine Coating Systems (Reapproved 2011), Standard Test Method. West Conshohocken, PA, United States.
<https://doi.org/10.1520/D6990-05.2>
- E.U. Copernicus Marine Service Information, 2020. Baltic Sea physics analysis and forecast [WWW Document]. URL
https://resources.marine.copernicus.eu/?option=com_csw&view=details&product_id=BALTICSEA_ANALYSIS_FORECAST_PHY_003_006 (accessed 11.5.20).
- Earley, P.J., Swope, B.L., Barbeau, K., Bundy, R., McDonald, J. a, Rivera-Duarte, I., 2014. Life cycle contributions of copper from vessel painting and maintenance activities. *Biofouling* 30, 51–68. <https://doi.org/10.1080/08927014.2013.841891>
- Holtrop, J., Mennen, G.G.J., 1982. An approximate power prediction method. *Int. Shipbuild. Prog.* <https://doi.org/10.1007/s13398-014-0173-7.2>
- IHS Markit, 2020. Sea-web Ships: detailed records on 200,000+ ships of 100 GT and above, updated nightly [WWW Document]. URL <https://maritime.ihs.com/> (accessed 10.28.20).
- IMO, 2020. Reduction of GHG emissions from ships - Fourth IMO GHG Study 2020 - Final Report [WWW Document]. MEPC 75/7/15.
<https://doi.org/10.1017/CBO9781107415324.004>
- ISO, 2016. ISO 19030:2016 - Ships and marine technology - Measurement of changes in hull and propeller performance [WWW Document]. ISO/TC 8/SC 2. URL
http://www.iso.org/iso/home/store/catalogue_tc/catalogue_detail.htm?csnumber=63774 (accessed 6.1.17).
- Jalkanen, J.P., Brink, A., Kalli, J., Pettersson, H., Kukkonen, J., Stipa, T., 2009. A modelling system for the exhaust emissions of marine traffic and its application in the Baltic Sea area. *Atmos. Chem. Phys.* 9, 9209–9223.
<https://doi.org/10.5194/acp-9-9209-2009>
- Kowalski, A., 2020. The impact of the underwater hull anti-fouling silicone coating on a ferry's fuel consumption. *J. Mar. Sci. Eng.* 8. <https://doi.org/10.3390/jmse8020122>
- Lagerström, M., Ytreberg, E., Wiklund, A.K.E., Granhag, L., 2020. Antifouling paints leach copper in excess – study of metal release rates and efficacy along a salinity gradient. *Water Res.* 186. <https://doi.org/10.1016/j.watres.2020.116383>
- Leer-Andersen, M., 2018. Slutrapport för “Ytfriktionsdatabas för maritima sektorn” [RE40147243-02-00-A]. Gothenburg.
- Naval Sea Systems Command, 2006. Chapter 081 – Water-borne underwater hull cleaning of Navy ships, in: *Naval Ship's Technical Manual*. Washington DC.
- Noring, M., Håkansson, C., Dahlgren, E., 2016. Valuation of ecotoxicological impacts from tributyltin based on a quantitative environmental assessment framework. *Ambio* 45, 120–129. <https://doi.org/10.1007/s13280-015-0682-4>
- Oliveira, D.R., Granhag, L., 2020. Ship hull in-water cleaning and its effects on fouling-control coatings. *Biofouling* 36, 332–350.
<https://doi.org/10.1080/08927014.2020.1762079>
- Oliveira, D.R., Granhag, L., Larsson, L., 2020. A novel indicator for ship hull and

- propeller performance: Examples from two shipping segments. *Ocean Eng.* 205. <https://doi.org/10.1016/j.oceaneng.2020.107229>
- Schultz, M.P., Bendick, J.A., Holm, E.R., Hertel, W.M., 2011. Economic impact of biofouling on a naval surface ship. *Biofouling* 27, 87–98. <https://doi.org/10.1080/08927014.2010.542809>
- Valkirs, A.O., Seligman, P.F., Haslbeck, E., Caso, J.S., 2003. Measurement of copper release rates from antifouling paint under laboratory and in situ conditions: Implications for loading estimation to marine water bodies. *Mar. Pollut. Bull.* 46, 763–779. [https://doi.org/10.1016/S0025-326X\(03\)00044-4](https://doi.org/10.1016/S0025-326X(03)00044-4)
- Woud, H.K., Stapersma, D., 2016. Design of propulsion and electric power generation systems. IMarEST, London.
- Yeginbayeva, I.A., Atlar, M., 2018. An experimental investigation into the surface and hydrodynamic characteristics of marine coatings with mimicked hull roughness ranges. *Biofouling* 34, 1001–1019. <https://doi.org/10.1080/08927014.2018.1529760>
- Ytreberg, E., Åström, S., Fridell, E., 2021. Valuating environmental impacts from ship emissions – The marine perspective. *J. Environ. Manage.* 282.